J Ther Eng, Vol. 10, No. 3, pp. 638−656, May, 2024

Journal of Thermal Engineering
Web page info: https://jten.yildiz.edu.tr
DOI: 10.14744/thermal.0000816

Research Article

Numerical study on heat transfer and fluid dynamics in plate heat exchangers: Effects of chevron angle and aspect ratio

Sami KAPLAN[1], Kubilay BAYRAMOĞLU[2], Mehmet SARIKANAT[1], Lütfiye ALTAY[1]

[1]Department of Mechanical Engineering, Ege University, Izmir, 35100, Türkiye
[2]Department of Marine Engineering, Zonguldak Bulent Ecevit University, Zonguldak, 67100, Türkiye

ARTICLE INFO

Article history
Received: 11 November 2022
Accepted: 02 March 2023

Keywords:
Aspect Ratio; Chevron Angle; Computational Fluid Dynamics (CFD); Friction Factor; Heat Transfer; Nusselt Number; Plate Heat Exchanger; Thermohydraulic Performance; Turbulence Enhancement

ABSTRACT

Determination of the geometrical parameters of the heat exchanger has important effects on the thermohydraulic performance of the heat exchanger. In this study, the effects of geometric parameters of a plate heat exchanger on thermohydraulic performance have been extensively investigated using computational fluid dynamics (CFD). Parametric studies were performed on 8 different corrugated channel geometries with various chevron angles (β) and aspect ratios (2b/λ) for Reynolds numbers ranging from 500 to 3000. An entire fluid channel was numerically studied using the same mass flow rate and the Reynolds number. As results of the study, temperature distribution, pressure gradient, velocity, turbulent kinetic energy distribution, Nusselt number, friction factor, and flow properties were evaluated comparatively for each case. It was determined that the sinusoidal corrugations promote the turbulence intensity and the swirling flow which leads to thermal boundary layer mitigation and enhanced convection heat transfer in response to the increasing of aspect ratio. The results of the study show that the (CFD) model is a reasonable and effective technique for displaying 3D contour plots, streamlines, and determining performance parameters.

Cite this article as: Kaplan S, Bayramoğlu K, Sarıkanat M, Altay L. Numerical study on heat transfer and fluid dynamics in plate heat exchangers: Effects of chevron angle and aspect ratio. J Ther Eng 2024;10(3):638−656.

INTRODUCTION

The main parameters affecting the development of heat exchangers are economy, thermal efficiency, compactness, and lightweight [1]. Plate heat exchangers are among the most important and comprehensive equipment in the industry as they provide the required efficient heat transfer for industrial processes. Heat exchangers allow both easy service and maintenance and flexible design parameters [2]. Plate heat exchangers are generally used in heating, cooling, waste heat recovery systems, condensers, and evaporators. Compared to shell and tube heat exchangers, plate heat exchangers allow high turbulence and are commonly used for liquid-to-liquid heat transfer [3]. However, plate heat exchangers have a more complex geometry compared to other heat exchangers due to the increase in the heat transfer area and turbulence rate in order to increase the

***Corresponding author.**
*E-mail address: kubilay.bayramoglu@beun.edu.tr

This paper was recommended for publication in revised form by Editor-in-Chief Ahmet Selim Dalkılıç

thermal performance [4]. When designing heat exchangers, some basic parameters such as Nusselt number and friction factor should be obtained. Therefore, various methods and techniques are applied to obtain the basic parameters that are effective in the performance of the heat exchanger [5]. In optimum heat exchanger design, there must be a balance between friction losses and heat transfer. Therefore, the designer should ensure the appropriate selection of parameters that balance these two factors for optimum performance [1]. Various studies have been carried out in the literature on the parameters affecting the plate heat exchanger performance.

Gullapalli and Sundén, [6] investigated the thermal and hydraulic characteristics of the small fluid sections in a plate heat exchanger using experimental and numerical work. In parametric studies performed at 300-3000 Reynolds numbers, heat transfer and pressure drop were underestimated by 20-30% and 10-35%, respectively. Kanaris et al. [7] numerically performed the heat transfer and fluid flow calculations in a corrugated plate heat exchanger with CFD code. In this study, friction factor and Nusselt number were determined for various Reynolds numbers. Septet et al. [8] examined the heat transfer coefficient of the plate heat exchanger fabricated by additive manufacturing with an experimental study. In an experimental study, flow boiling, and condensation were conducted and n-heptane and water were used as heat transfer fluids. The thermohydraulic characteristics were determined using infrared thermography. Gherasim et al. [9] compared the thermal and hydraulic characteristics of the two-channel plate heat exchanger by experimental and numerical analysis. The analyses were carried out with the hot and cold fluid Reynolds numbers less than 400, and the friction factor and Nusselt number were determined. Yang et al. [10] experimentally investigated the effect of different geometric parameters on heat transfer for nine brazed plate heat exchangers. A mixture of ethylene glycol and water was used as the working fluid in this study. The results of the study showed that the herringbone angle is the most effective parameter on the thermal performance of the heat exchanger. In addition, individual correlation and general correlation studies obtained from experimental data were carried out in their studies. Khan et al. [11] investigated the effect of different chevron angles and corrugation depths on thermal performance in two symmetrical and mixed plate configurations. An experimental study was carried out at 500-2500 Reynolds numbers and 3.5-6.5 Prandtl numbers. The results of the study showed that the Reynolds number and chevron angle could significantly affect the heat transfer coefficient. Gherasim et al. [12] determined the friction factor, Nusselt number, and isotherm characteristics experimentally at the inlet and outlet of the chevron-type plate heat exchanger for laminar and turbulent flow conditions. Arsenyeva et al. [13] determined the minimum heat transfer area for the pressure drop, temperature distribution, stream physical properties, and heat load on the plate heat exchanger with a mathematical model. They demonstrated the importance of choosing geometric parameters to design heat exchangers of different sizes and geometric forms for different heat transfer process conditions with the mathematical model. In addition, various studies were carried out on the optimization of the plate heat exchanger design and operation parameters. Wang et al. [14] presented a method for optimizing the heat exchanger network (HEN) for plate heat exchangers, and Longo et al. [15] presented the artificial neural network (ANN) method for determining the total heat transfer. Fernández-Seara et al. [16] investigated numerous parametric studies on the use of the Wilson method and the modified Wilson method to determine the thermal performance of the plate heat exchanger. Lotfi and Sundén [17] numerically evaluated the design of a finned and elliptical tube heat exchanger as a novel type of geometry such as tube-banks, namely slotted elliptical tube-banks (SETBs) and slotted annular elliptical tube-banks (SAETBs). Han et al. [18] numerically investigated the Nusselt number, friction factor and design optimization on a double sinusoidal plate heat exchanger. Tsai et al. [19] examined the hydrodynamic parameters of the plate heat exchanger experimentally and numerically. The pressure drop obtained from the numerical study has been verified with the experimental data. Aradag et al. [20] investigated the Nusselt number and friction factor of gasketed plate heat exchanger, which is small in volume, easy to clean and has high thermal performance, with ANN. Khan et al. [11] evaluated the heat transfer coefficient change of the plate heat exchanger in the range of 500-2500 Reynolds number and 3.5-6.5 Prandtl number in the range of different chevron angles. Gherasim et al. [12] experimentally investigated the hydraulic and thermal characteristics of a channel chevron type heat exchanger for laminar and turbulent flow conditions.

Most of those given in literature have studied the effect of limited geometric parameters of the plate heat exchanger on convection heat transfer [5, 21, 22]. In this study, the extensive geometrical characteristics and flow properties of the plate heat exchanger were investigated numerically under the same flow conditions and the Reynolds number. The numerical model was performed in 3D with the computational fluid dynamics model and the boundary conditions of the numerical model were verified with the literature data. In the validated model, geometric parameters such as chevron angle, corrugation length, and operation parameters such as mass flow rate and Reynolds number were compared for different conditions.

In this study, a detailed numerical analysis was carried out to establish a meaningful relationship between the geometric parameters of plate heat exchangers and their thermo-hydraulic performance and flow structure. In addition, flow characteristics such as fluid temperature, pressure, velocity, and streamline are presented comparatively for different conditions on the 3D model. Thus, unlike other studies, this study will make significant contributions to the

literature in terms of providing a comprehensive parametric study on turbulent kinetic energy distribution, streamlines, planar and axial temperature distribution, and thermal boundary layer for the corrugated plate heat exchangers.

METHODOLOGY

Model Description

In this study, the 3D model of the plate heat exchanger was numerically modeled. Figure 1 represents the solid model of the heat exchanger. In the given model, chevron angle, wavelength, and flow regions are represented in Figures 1a, 1b, and 1c, respectively.

Flow boundaries were modeled with Ansys Spaceclaim as 125 * 70 mm for L_W and L_{Ch}, respectively. Parametric studies were carried out at two different chevron angles and four variable aspect ratios, giving the relationship between wavelengths and heights. The chevron angle (β) was chosen as 30 ° and 60 ° and the aspect ratio (ϒ) was chosen as 0.4, 0.6, 0.8 and 1.33. In addition, the flow conditions were turbulent at Reynolds numbers between 500 and 3000. The geometric parameters chosen are based on the commercial size in the market for plate heat exchangers. Geometric parameters are shown in Table 1.

Numerical Setup

The numerical model consists of structural elements with Fluent meshing of approximately 2M elements. The numerical model network structure is presented in Figure 2.

According to the mesh independency test, at 2M structural element with 10 layers of poly-prism mesh, the numerical model was independent of the number of elements, in which case the calculated Y+ value by Ansys Fluent was 1.3.

The mesh is modeled with a boundary layer consisting of 10 layers of poly-prism mesh in all flow regions and poly-hexcore volume mesh. Ansys Fluent automatic mosaic mesh technology, conformally combines high-quality polyhedral boundary layer mesh with hexahedron volume mesh

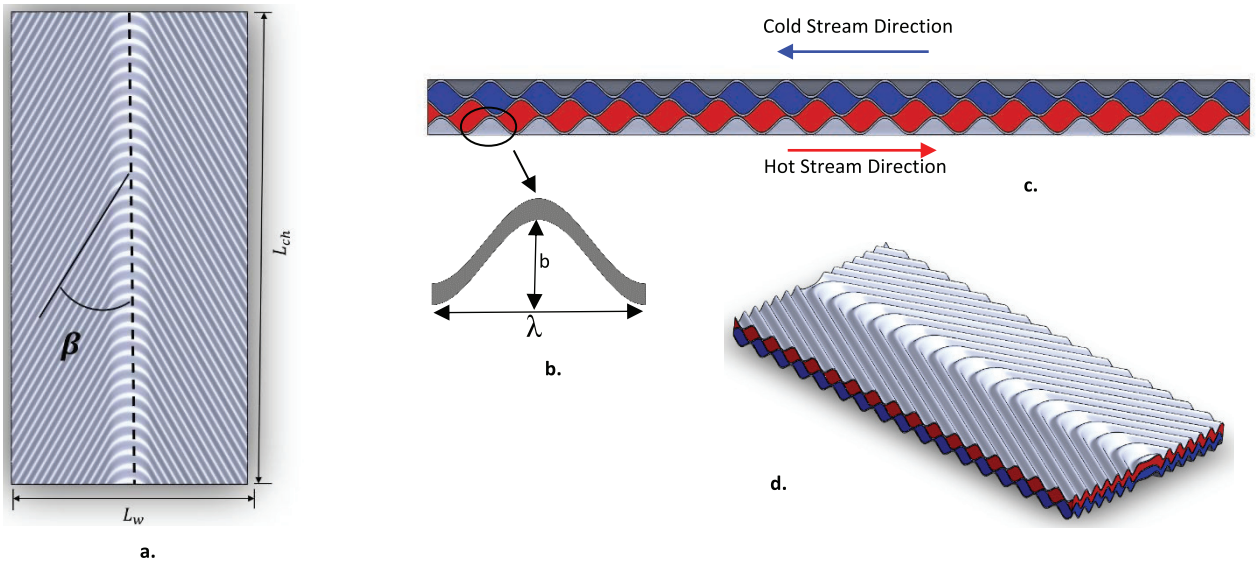

Figure 1. 3D model of the heat exchanger.

Table 1. Geometric parameters of heat exchanger

Geometry Name	ß [°]	ϒ(2b/λ)	Plate Surface area [mm²]	ϕ
2_6_30	30	0.66	4133.52	1.65
2_6_60	60	0.66	3235.16	1.29
2_10_30	30	0.40	3214.83	1.29
2_10_60	60	0.40	2795.64	1.12
4_6_30	30	1.33	6792.80	2.72
4_6_60	60	1.33	4684.64	1.87
4_10_30	30	0.80	4652.55	1.86
4_10_60	60	0.80	3501.72	1.40

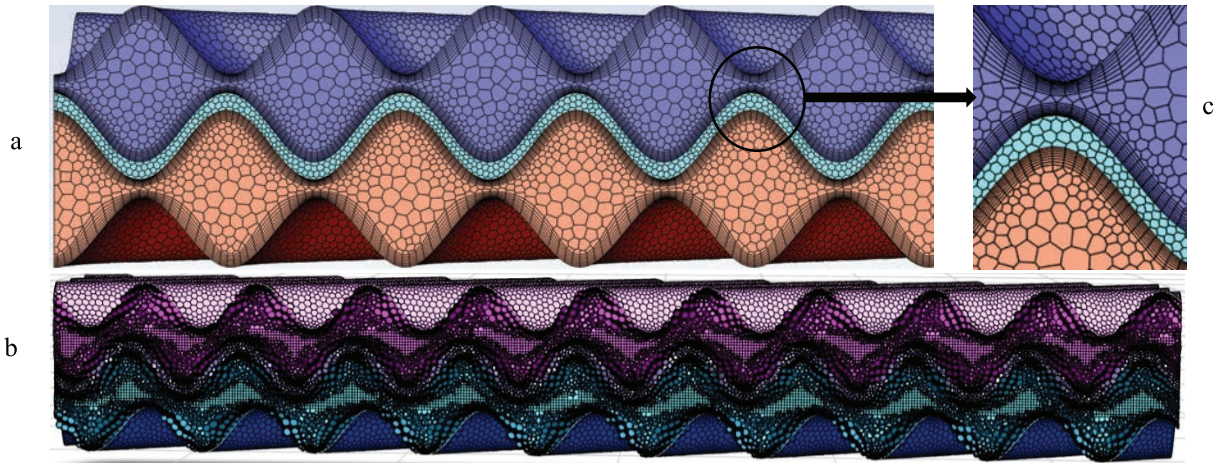

Figure 2. Fluid and solid poly-hexcore meshes with poly-prism boundary layer mesh a) surface mesh b) cross-sectional poly-hexcore volume mesh c) close view of boundary layer mesh.

elements. In this technology the bulk region is meshed with octree hexahedral elements. The boundary layer is filled with isotropic poly-prisms and the transition region is meshed with mosaic polyhedral elements [23].

In the model, enhanced wall treatment wall functions have been used. The enhanced wall treatment is a blended wall pattern or wall function. It blends the separate models in the two-layer approach, using a damping function to make the transition between the two smoother [24]. The mesh independence analysis is given in Figure 3. Mesh independency analysis was performed at 3000 Reynolds numbers with chevron angle and aspect ratio being 30 and 0.8, respectively. Also, the Nusselt number was compared for each element number.

In this study, the flow is modeled as turbulent. The flow characteristics in plate heat exchangers, is determined by the Reynolds number. For laminar flow, the Reynolds number is less than 200. Hence the Reynolds number for the k-e turbulence model is more than 200 [25]. The RANS-based 2-equation k-ε turbulence model was chosen. The 2-equation turbulence model gives more accurate results than other models in defining of both boundary layer and wall functions in heat exchangers [7, 15]. In addition, the RNG k-ε model used in this study is a relatively inexpensive two-equation model that describes the eddy viscosity as a function of turbulent kinetic energy and turbulent propagation velocity and is often used in similar applications [6]. To combine the two-layer model with enhanced wall

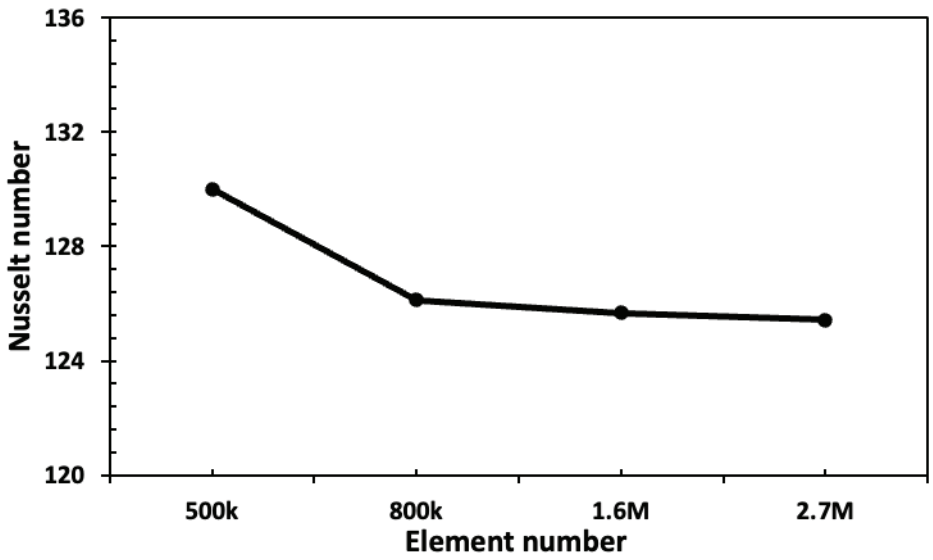

Figure 3. Mesh independency test.

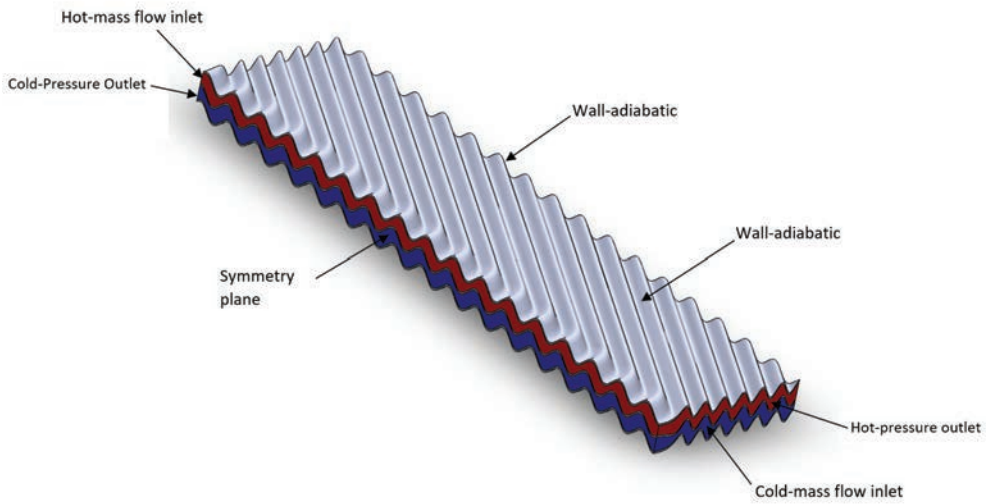

Figure 4. Boundary conditions.

Table 2. Boundary conditions

Boundary Conditions			Units	Value or specification
Inlet	Hot	Mass flow inlet	kg/s	Variable based on Reynolds
		Temperature	K	333.15
		Turbulence intensity	%	5
	Cold	Mass flow inlet	kg/s	Variable based on Reynolds
		Temperature	K	303.15
		Turbulence intensity	%	5
Outlet		Pressure outlet	atm	Atmospheric pressure
Walls		Outer walls	-	Adiabatic wall-no slip
		Intermediate walls	-	Coupled wall-no slip

functions, enhanced wall treatment near wall modeling method has been used which results in better agreement with the experimental data [24]. The heat transfer calculation between the cold and hot fluid is provided by the conservation of energy. The numerical model boundary conditions are presented in Figure 4.

The model consists of the boundary conditions of hot and cold inlet mass flow rates, where hot and cold streams enter the system. The outlets are defined as pressure outlets. In addition, the input boundary condition is defined as the temperature input as well as the mass flow rate. The upper and lower metal walls of the heat exchanger are defined as the adiabatic wall. The intermediate metal plate between the hot and cold streams was defined as a coupled wall. Table 2 shows the model boundary conditions.

Governing Equations

The numerically realized model with CFD is governed by the equations of continuity, momentum, and energy. The continuity equation, also known as the conservation of mass, is expressed as Eq. (1).

$$\frac{\partial \rho}{\partial t} + \nabla(\rho \vec{v}) = 0 \quad (1)$$

where ρ is density and v is velocity. The momentum equation, also known as the Navier-Stokes equations, is given in Eq. (2).

$$\frac{\partial}{\partial t}(\rho \vec{v}) + \nabla \cdot (\rho \vec{v} \vec{v}) = -\nabla P + \nabla \cdot \tau + \rho \vec{g} \quad (2)$$

Where, P is the static pressure, τ is the stress tensor and $\rho \vec{g}$ is the gravitational body force. Conservation of energy is described by Eq. (3) [26].

$$\frac{\partial}{\partial t}(\rho E) + \nabla \cdot [\vec{v}(\rho E + P)] = \nabla \cdot (k_t \nabla T + \tau \cdot \vec{v}) \quad (3)$$

Where k_t is the thermal conductivity and E is defines as total energy per mass units for incompressible flows [27].

The two equations governing the RNG K-E turbulence model, and the wall laws are described by Eq. (4) and Eq. (5), respectively [14].

$$\frac{\partial}{\partial_t}(\rho k)+\frac{\partial}{\partial_{x_i}}(\rho k v_i)=\frac{\partial}{\partial_{x_i}}\left(\alpha_k v_{eff}\frac{\partial_k}{\partial_{x_i}}\right)+G_k+G_b-\rho\varepsilon-Y_M+S_k \quad (4)$$

$$\frac{\partial}{\partial_t}(\rho\varepsilon)+\frac{\partial}{\partial_{x_i}}(\rho k v_i)=\frac{\partial}{\partial_{x_i}}\left(\alpha_\varepsilon v_{eff}\frac{\partial_\varepsilon}{\partial_{x_j}}\right)+G_{1\varepsilon}\frac{\varepsilon}{k}(G_k+C_{3\varepsilon}G_b) - G_{2\varepsilon}\rho\frac{\varepsilon^2}{k}-R_\varepsilon+S_\varepsilon \quad (5)$$

In these equations, G_k represents the generation of turbulence kinetic energy due to the mean velocity gradients, calculated as described in Modeling Turbulent Production in the k-ε Models. G_k is the generation of turbulence kinetic energy due to buoyancy, calculated as described in Effects of Buoyancy on Turbulence in the k-ε Models. Y_M represents the contribution of the fluctuating dilatation in compressible turbulence to the overall dissipation rate, calculated as described in Effects of Compressibility on Turbulence in the k-ε Models. The quantities α_k and α_ε are the inverse effective Prandtl numbers for k and ε, respectively. S_k and S_ε are user-defined source terms.

The Reynolds number can be obtained from Eq. (6) for the plate heat exchanger.

$$Re=\frac{G\cdot D_h}{\mu} \quad (6)$$

In the Eq. (6), Re is Reynolds number, G is the mass flux or mass velocity, μ is the viscosity, and D_h is the hydraulic diameter. Mass flux or mass velocity can be expressed by Eq. (7),

$$G=\frac{\dot{m}}{L_w\cdot(D_e/2)} \quad (7)$$

where L_w is the plate width and $\dot{m}$ mass flow. In the plate heat exchanger, the friction coefficient is determined with Darcy-Weisbach Eq. (8).

$$f=\Delta P_f\cdot {A_{ch}}^2\cdot\left(\frac{D_h}{2}\right)\cdot 2\cdot\left(\frac{\rho}{\dot{m}^2}\right) \quad (8)$$

Overall heat transfer coefficient (U) can be calculated by Eq. (9)-Eq. (11) [25].

$$U=\frac{Q_m}{A\cdot LMTD} \quad (9)$$

$$LMTD=\frac{(T_{h,i}-T_{c,o})-(T_{h,o}-T_{c,i})}{\ln\left(\frac{T_{h,i}-T_{c,o}}{T_{h,o}-T_{c,i}}\right)} \quad (10)$$

$$\frac{1}{U}=\frac{1}{h_h}+\frac{1}{h_c}+\frac{t}{k} \quad (11)$$

As mentioned above, the Reynolds number was kept the same on both sides of the plate during the experiment, such that the heat transfer coefficient on both sides was assumed to be the same, ie $h_c = h_h = h$; therefore, Eq. (10) can be written as [29]:

$$\frac{1}{h}=\frac{1}{2}\left(\frac{1}{U}-\frac{t}{k}\right) \quad (12)$$

Where h_h is hot stream convection coefficient, h_c is cold stream convection coefficient and $\frac{t}{k}$ is the conduction resistance.

Validation

Validation of numerical models with experimental or literature data and selection of appropriate boundary conditions are important for the accuracy of the study. A

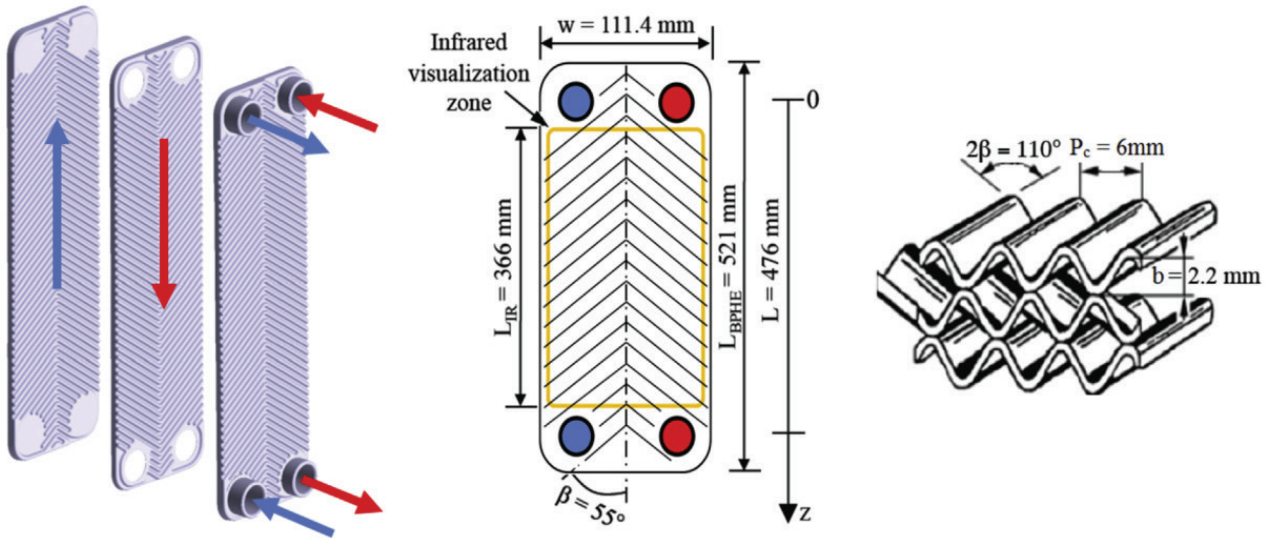

Figure 5. Validated model.

Table 3. Boundary condition for validation

Boundary Conditions			Units	Value or specification
Inlet	Hot	Mass flow inlet	kg/s	Variable based on Reynolds
		Temperature	K	333.15
	Cold	Mass flow inlet	kg/s	Variable based on Reynolds
		Temperature	K	303.15
Outlet		Pressure outlet	atm	Atmospheric pressure
Walls		Outer walls	-	Adiabatic wall-no slip
		Intermediate walls	-	Coupled wall-no slip

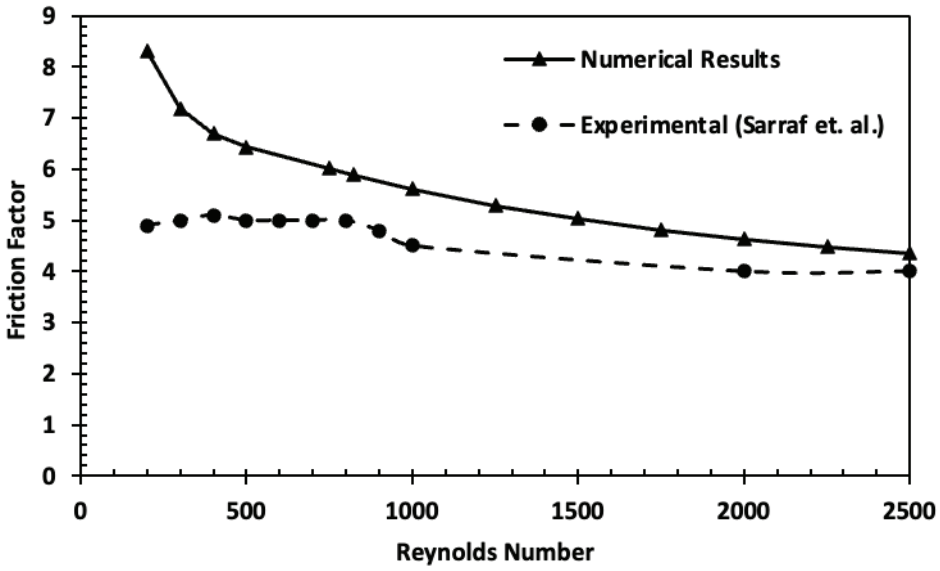

Figure 6. Validation of numerical model.

numerical model validation study was conducted with the data obtained from the literature [25]. The numerical model used in the validation study is given in Figure 5.

The boundary conditions used in the validation study are given in Table 3. The given boundary conditions are the experimental operating boundary conditions and are the same as the numerical boundary conditions and geometric parameters used in the validation.

The variation of the friction factor with the Reynolds number obtained by numerical and experimental studies is given in Figure 6. As it is seen from Figure 6, the obtained results are compatible with each other. The maximum disagreement between the experimental and numerical simulation is 35% at Re=200, but the minimum disagreement between the numerical and experimental is 8.5 % at Re=2500. This indicates that the presented numerical simulation is in better agreement with experimental study for the flow regimes with higher Reynolds numbers.

RESULTS AND DISCUSSION

In this study, the geometric and flow properties of the heat exchanger were numerically investigated under the same flow conditions and Reynolds number. The flow characteristics of the plate heat exchanger were obtained by 3D numerical analysis. Evaluation of thermal and hydraulic performance is presented with varying geometric configurations and Reynolds numbers.

Evaluation of Thermal Performance

Variation of Nusselt number against Reynolds number for a viscous liquid (Pr= 6.3) with different aspect ratios and chevron angles have been presented in Figure 7. It is seen from Figure 7 that induced three-dimensional swirling flow by plate corrugation and chevron angle increases forced convection and the Nusselt number. Besides, corrugated plate geometry with chevron angle resulted in several times higher heat transfer coefficient and Nusselt number than flat-parallel geometry. Additionally, as can be seen from Figure 6, the effects of the corrugation aspect ratio (λ) and chevron angle (ß) on Nusselt number enhancement are

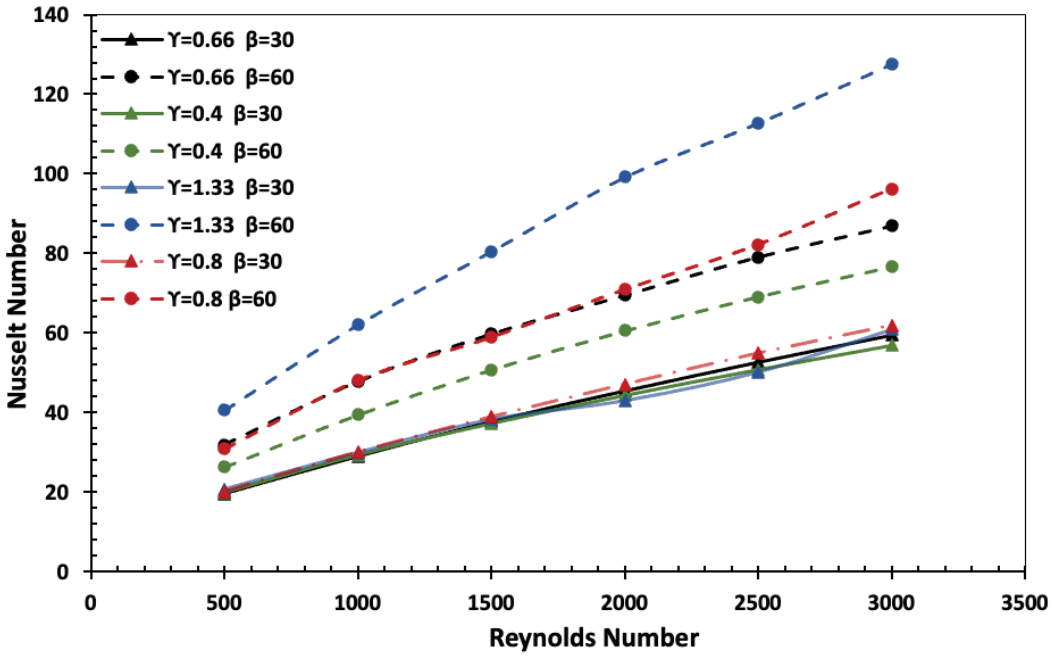

Figure 7. Variation of Nusselt number against Reynolds number for a viscous liquid (Pr=6.3) with different aspect ratios and chevron angles.

independent. For the aspect ratio of ϒ=1.33 and Re=2500, the Nusselt number at 60° chevron angle is twice as high as at 30°. Also, it should be noted that after a certain Reynolds number, the effect of the Reynolds number decreases due to the 3D swirling flow increase in the corrugated troughs, which is in agreement with Muley et al. [28]. For the aspect ratio of ϒ=1.33 and chevron angle of 60°, highest Nusselt numbers were obtained for all Reynolds numbers.

The variations of temperature gradients are shown in Figure 8 on the hot stream side of the intermediate plate for various corrugation aspect ratio and chevron angles. It can be clearly seen from Figure 8 that, the temperature decreases across the width of the plate as it approaches the symmetric axis of the plate. A similar trend can be seen in numerical work presented by [25]. This temperature gradient emerged as a consequence of two reasons. At first, the symmetric axis of the plate is where the tips of chevron angles come together and it has a more complex 3D swirling flow regime and more complex flow field geometry resulting in transverse vortices, a can be seen from 3D vector fields. This type of flow regime results in higher turbulent kinetic energy and low axial velocity, resulting in a higher Nusselt number and local heat flux. Also, lower axial velocity of fluid flow causes higher heat transfer rate. Another reason for the observed temperature gradient may be due to the uneven mass flow distribution in the flow field [14].

Variations of temperature gradients in the middle plane of the hot stream channel for various corrugation aspect ratios and chevron angles are shown in Figure 9. It can be seen from the Figure 9 that consistent results are obtained from the hot plate temperature distribution. The temperature at the centerline of the hot channel is generally lower than in the edge region, because of the higher turbulence rate, 3D swirling flow, and higher convection heat transfer rate.

The temperature distributions are demonstrated in Figure 10 for various corrugation aspect ratios and chevron angles in the direction of the main fluid flow. The results indicate that the slope of the temperature curve increases with the geometries with a higher aspect ratio and chevron angle for the same inlet Reynolds number which is in consistent with the result reported by [21]. The higher logarithmic mean temperature difference for geometries with higher aspect ratio and chevron angle can be explained by the higher turbulence and mixing swirling flow rate. The sinusoidal fluctuation of the curve emerges for two reasons. The first reason is the change in the distance of the probe line to the intermediate heat transfer corrugated plate, and the second reason is the highly mixing nature of the fluid flow.

The temperature distribution along the perpendicular direction to the heat exchanger plate (y-direction or flow direction) is demonstrated in Figure 11 for various corrugation aspect ratios and chevron angles. Kanaris et al. [1] demonstrated similar temperature profile in their numerical work. As can be seen from Figure 11, geometries with higher aspect ratio and chevron angle for the same inlet Reynolds number have a thermal boundary layer temperature profile with a steeper slope resulting in a narrower

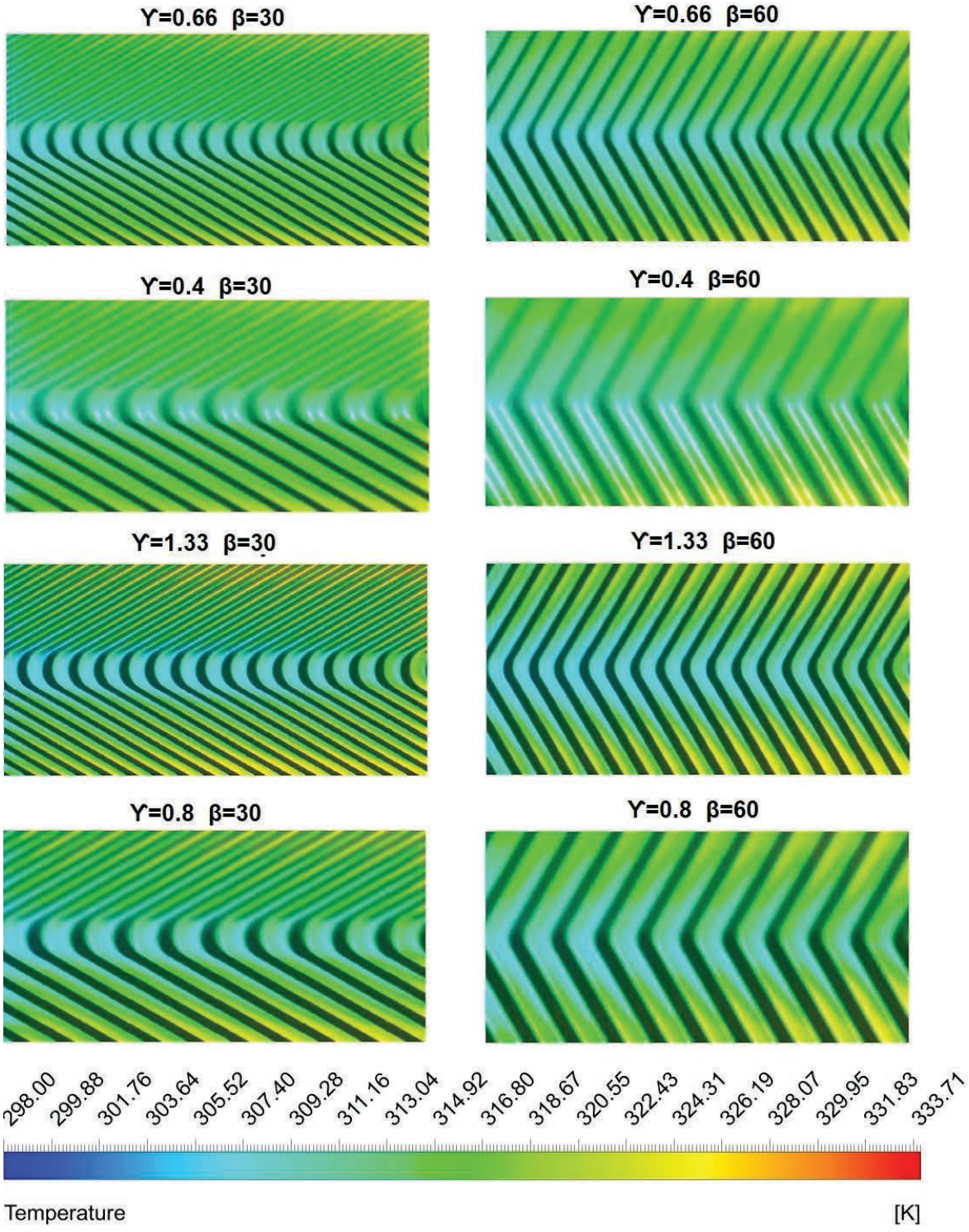

Figure 8. Temperature gradient on the hot stream side of the intermediate plate for various corrugation aspect ratios and chevron angles.

boundary layer. Also, intermediate wall temperatures (cold/hot) are lower for geometries with higher aspect ratio and corrugation angle which are caused by flows with higher mixing and turbulence rates.

Turbulent kinetic energy distributions are presented on the middle plane of the hot stream channel in Figure 12. Higher turbulence kinetic energy rates are observed with increasing chevron angle (ß) for the same Reynolds number

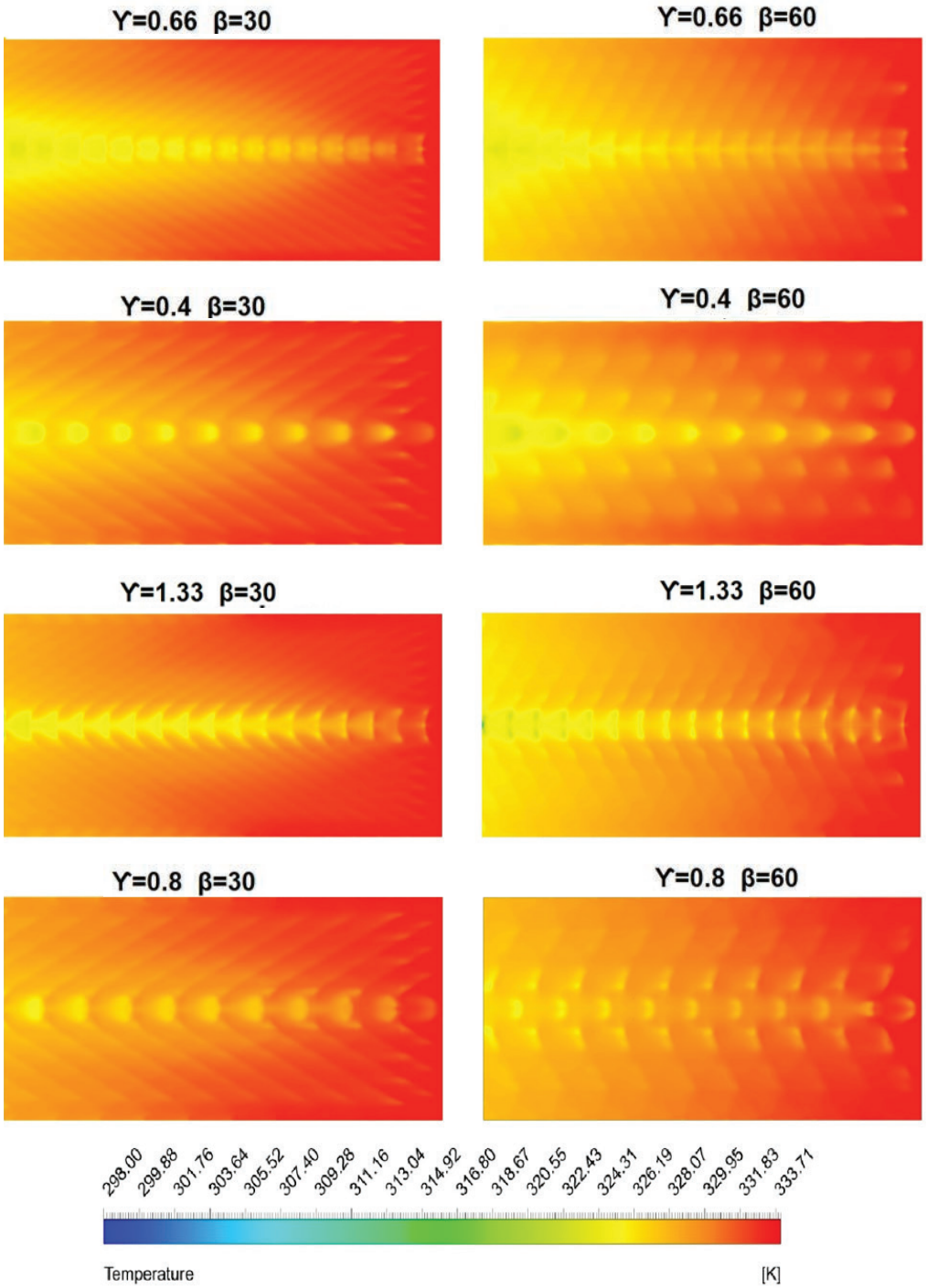

Figure 9. Temperature gradient on the middle plane of hot stream channel for various corrugation aspect ratios and chevron angles.

and aspect ratio indicating increased intensity of 3D swirl flow and transverse vortices generated by larger ß chevron plates. Besides, for the same Reynolds number and corrugation angle (ß), channels with higher aspect ratio values generate fluid flow with higher turbulence kinetic energy rate, which is due to greater 3D swirling flow. This is induced by deeper furrows, which also generate higher convection heat transfer rate and Nusselt number. However, higher friction losses and pressure drop also occurs. In addition, channels with a higher corrugation angle generate the faster (sooner) fully developed turbulent flow versus the lower chevron angle, behaviorally similar to the results by Lotfi and Sundén [17].

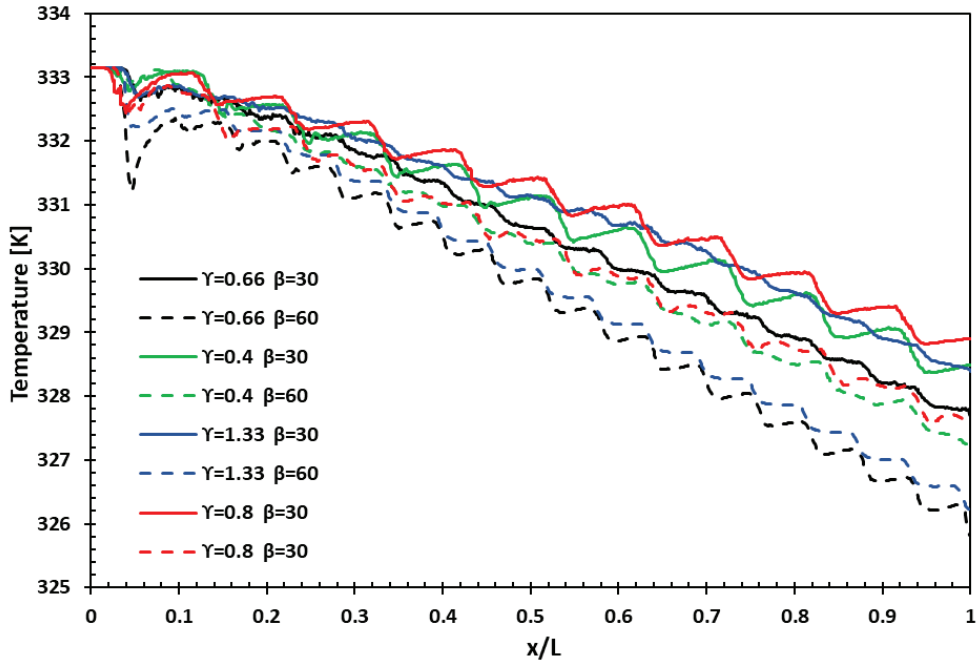

Figure 10. The temperature distributions for various corrugation aspect ratios and chevron angles in the direction of the main fluid flow.

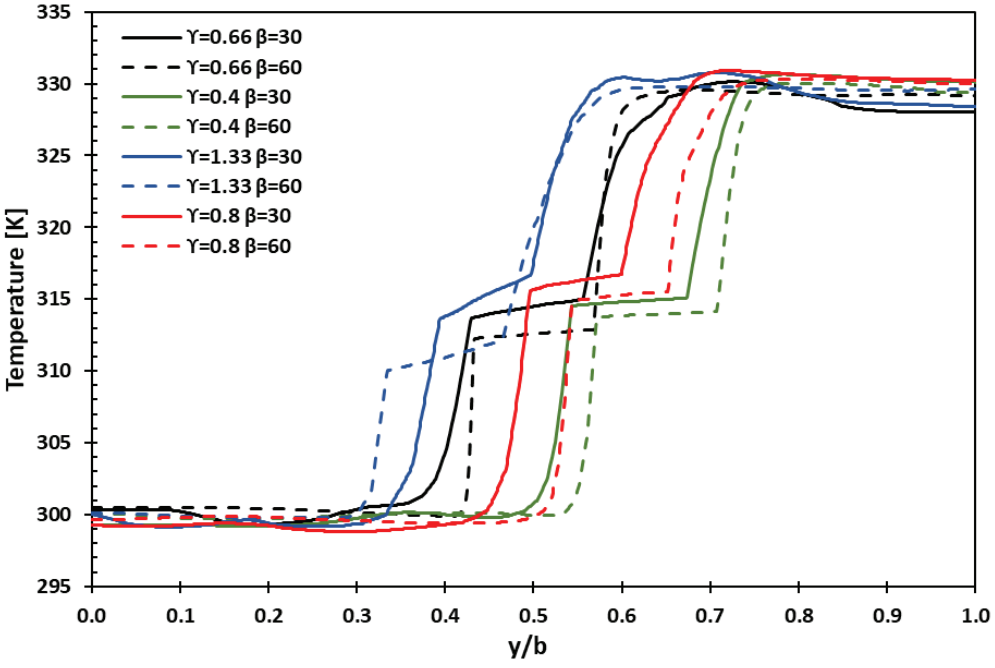

Figure 11. The temperature distributions for various corrugation aspect ratios and chevron angles perpendicular to the main flow direction.

Evaluation of Hydraulic Performance

Variation of isothermal friction factor against Reynolds number for various corrugation aspect ratios and chevron angles are demonstrated in Figure 13. The general trends of friction factor with Reynolds number are in agreement with the result of Muley et al. [28]. It can be deduced from the Figure 13 that increasing the plate aspect ratio Υ causes an increase in fanning friction factor. However, for geometries with the same aspect ratio, it is known that the one with a higher chevron angle has a greater friction factor,

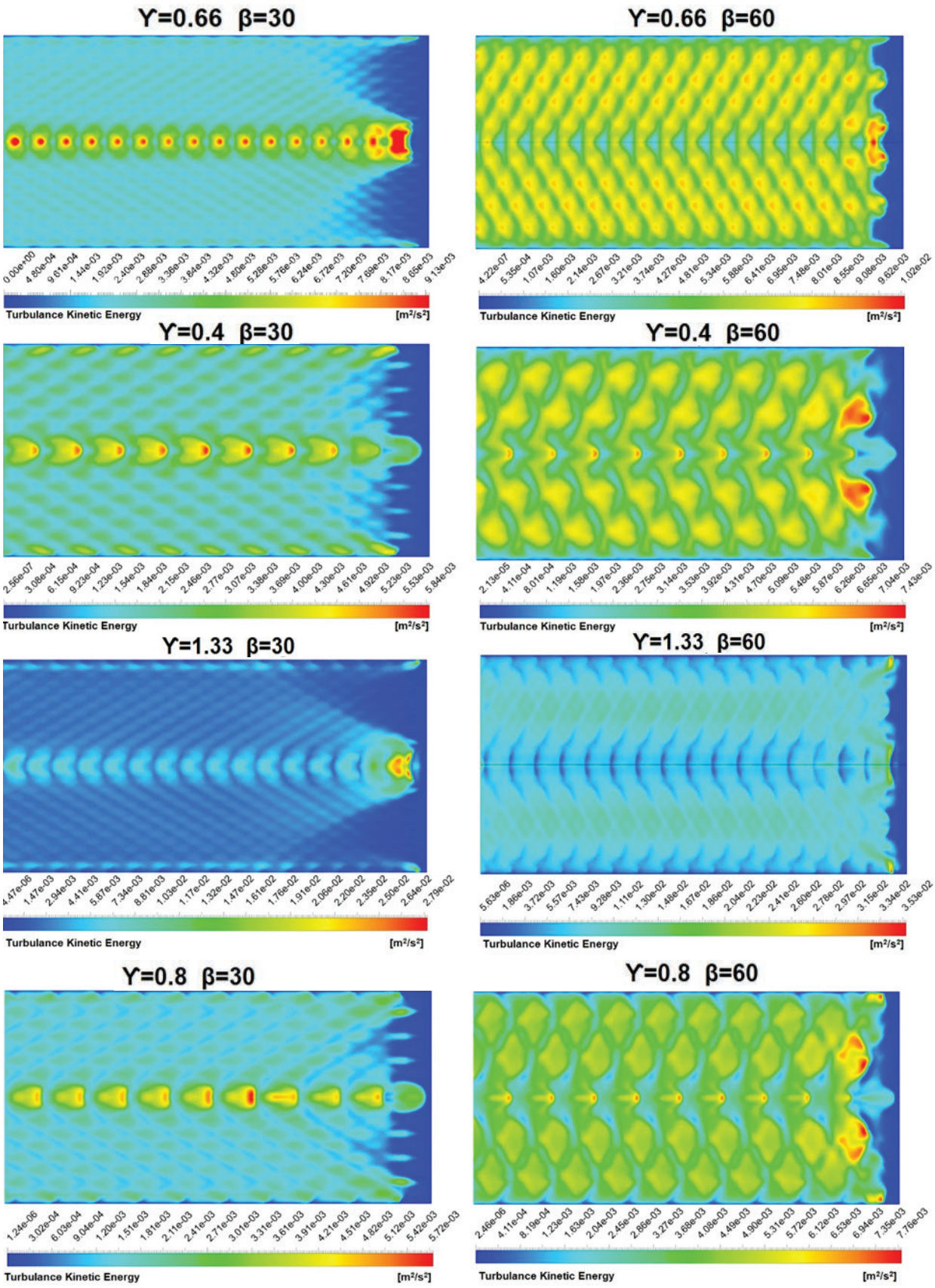

Figure 12. Turbulent kinetic energy distribution on the middle plane of hot stream channel for various corrugation aspect ratios and chevron angles.

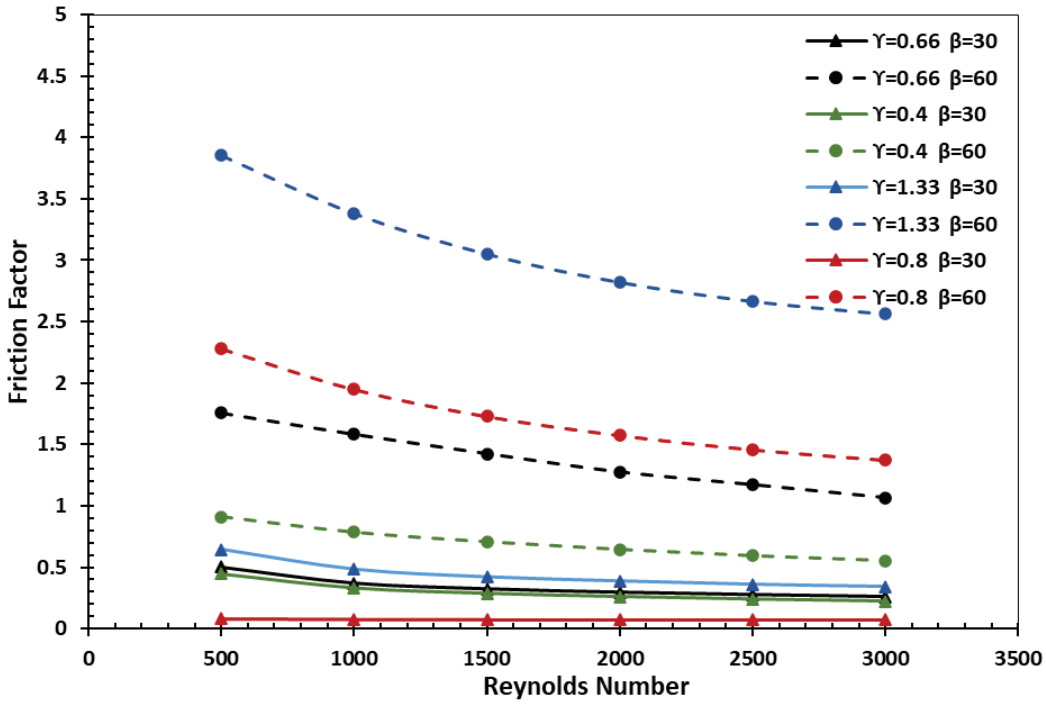

Figure 13. Variation of isothermal friction factor against Reynolds number for various corrugation aspect ratios and chevron angles.

indicating the chevron angle has a much more dominant effect on the friction factor than the aspect ratio. This is due to the fact that the plate with a higher chevron angle generates more intense transverse vortices in comparison to other lower chevron angles.

Also, with the increase of the Reynolds number, the establishment and development (growth) of 3D vortices in channel corrugates after a certain value of Reynold number leads to a change in the log-linear behavior of f-re, and increased amount of friction factor which is because of increased turbulent kinetic energy and therefore higher wall shear stress. However, at a lower Reynolds number, the increased friction factor for higher γ is primarily due to larger vortices and increased surface area. It should be noted that in comparison between two corrugated geometries with the same aspect ratio (γ), the geometry with a higher chevron angle has resulted in higher Nusselt number and friction factor, despite that the geometry with a lower chevron angle has a higher surface enlargement factor (ϕ). Therefore, the aspect ratio and chevron angle have a more significant effect on the thermo-hydraulic performance of plate heat exchangers. In other words, it can be said that the quality of turbulent flow and swirl flow generation is more effective than the surface area enlargement factor (ϕ). This result can be seen by comparing geometries of 1.33-30 and 1.33-60. 1.33-30 has the same aspect ratio (λ) as 1.33-60, and an even greater surface enlargement factor (ϕ) compared to the geometry of 1.33-60. However, the 1.33-60 geometry resulted in a higher Nusselt number value. In conclusion aspect ratio and chevron angle have a higher influence on turbulence and swirl flow generation than the surface enlargement factor.

Variations of pressure gradient, presented on the (Z=1/4 *Lw) plane for various corrugation aspect ratios and chevron angles in the direction of the main flow can be seen in Figure 14. One can see from the Figure 14 that geometry with a higher aspect ratio has a relatively steeper pressure gradient for the same Reynolds number and chevron angle. Besides, when the effect of aspect ratio on pressure gradient is evaluated, it is found that for the same Reynolds number and chevron angle, the channel with higher aspect ratio has greater flow friction due to the higher rate of momentum transfer and greater swirling fluid motion. Furthermore, there are some low-pressure regions on pressure gradient contour caused by the 3D swirling flow and vortices.

Evaluation of Flow Characteristics

Based on the numerical simulation applied in 8 different corrugated plate heat exchangers with Re=1500, 3D flow streamlines structure and velocities were obtained for various corrugation aspect ratios and chevron angles. There are two main flow patterns observed. The first flow regime concerns the fluid in the mid-plane of two plates following a helical flow structure in the main flow direction. The second flow structure relates to the fluid near the corrugated walls. This flow structure follows the corrugated paths to the ends and then passes to the other corrugated path on

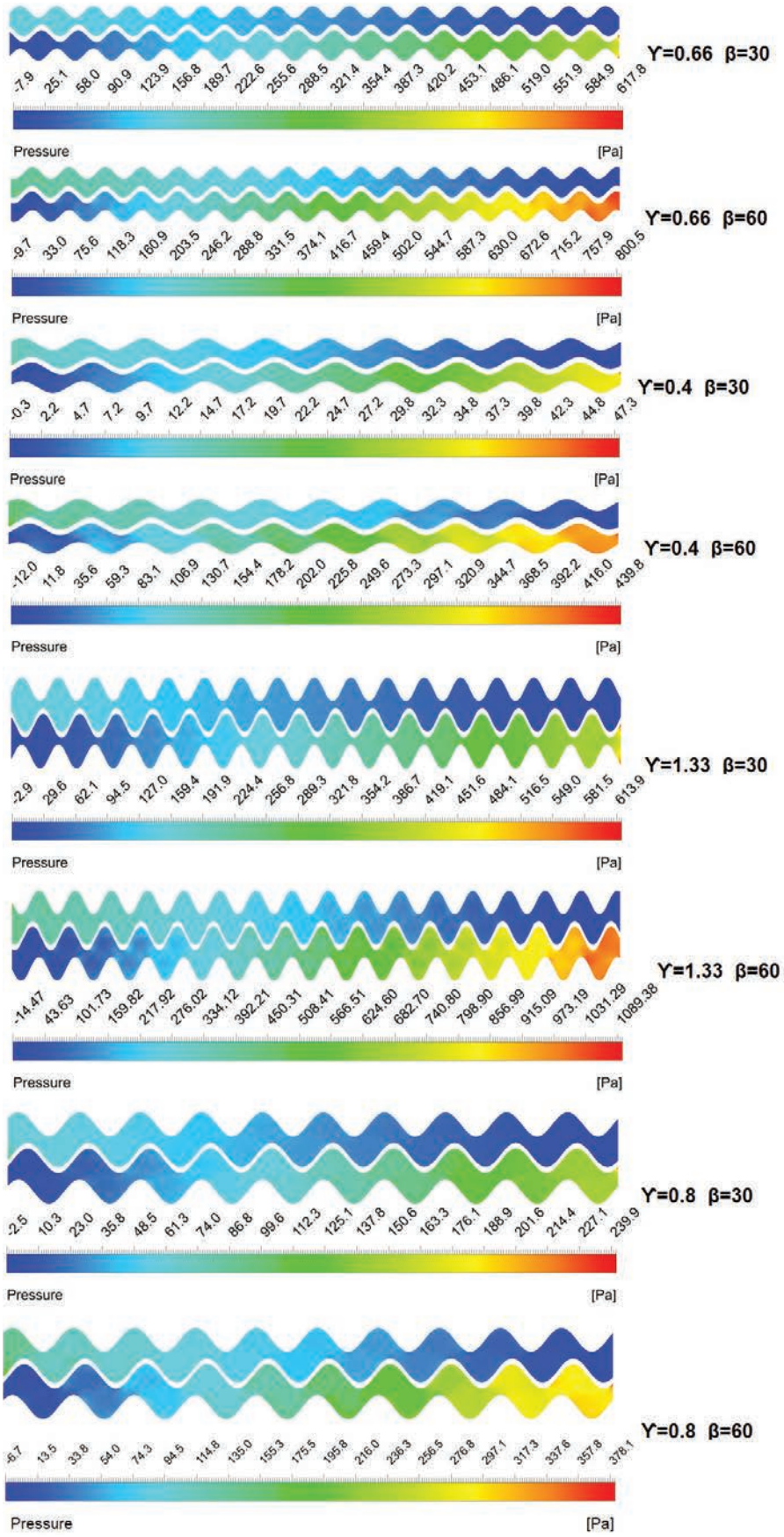

Figure 14. Pressure gradient in the direction of main flow for various corrugation aspect ratios and chevron angles.

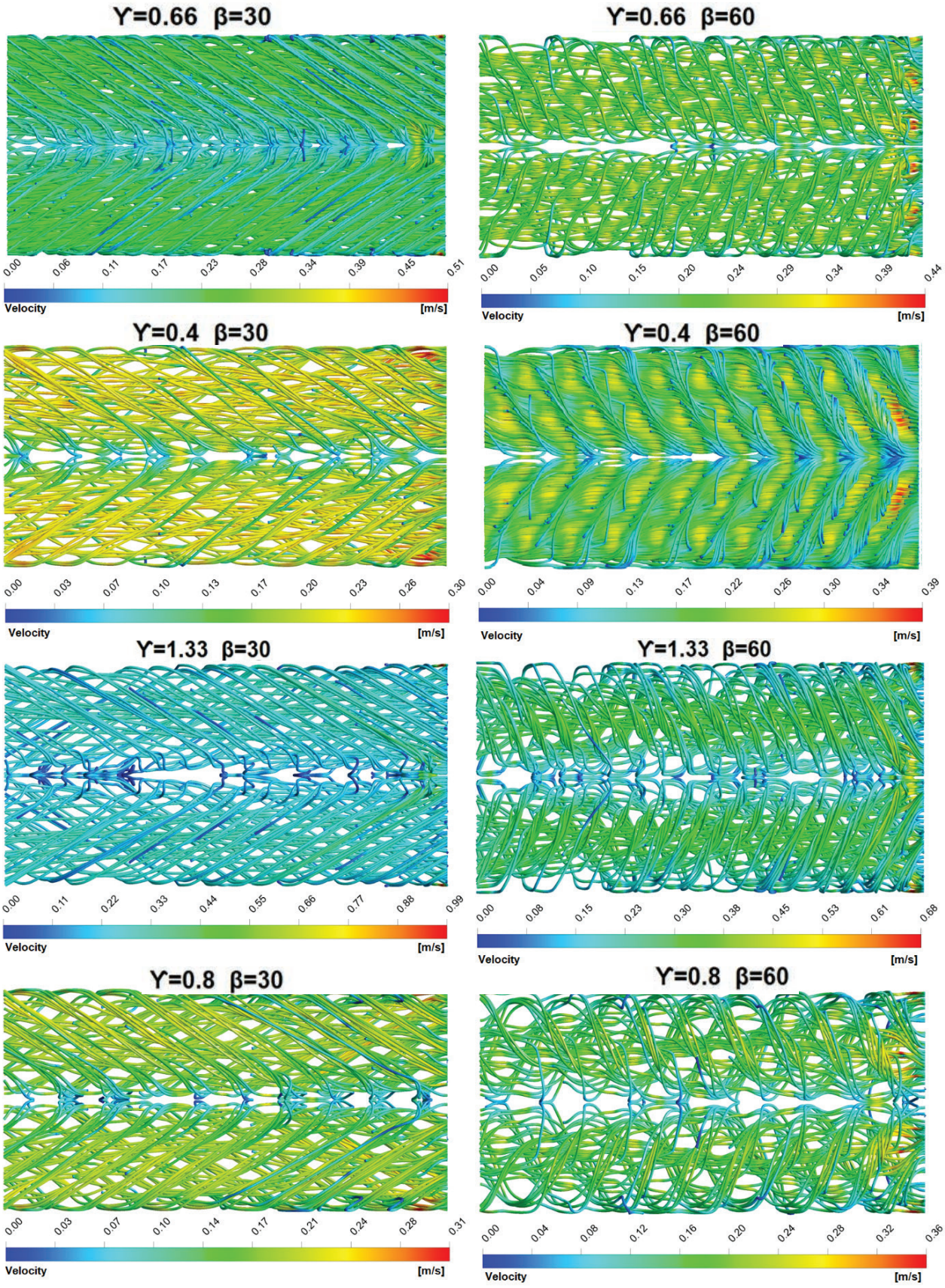

Figure 15. 3D flow streamlines structure and velocities for various corrugation aspect ratios and chevron angles with Re=1500.

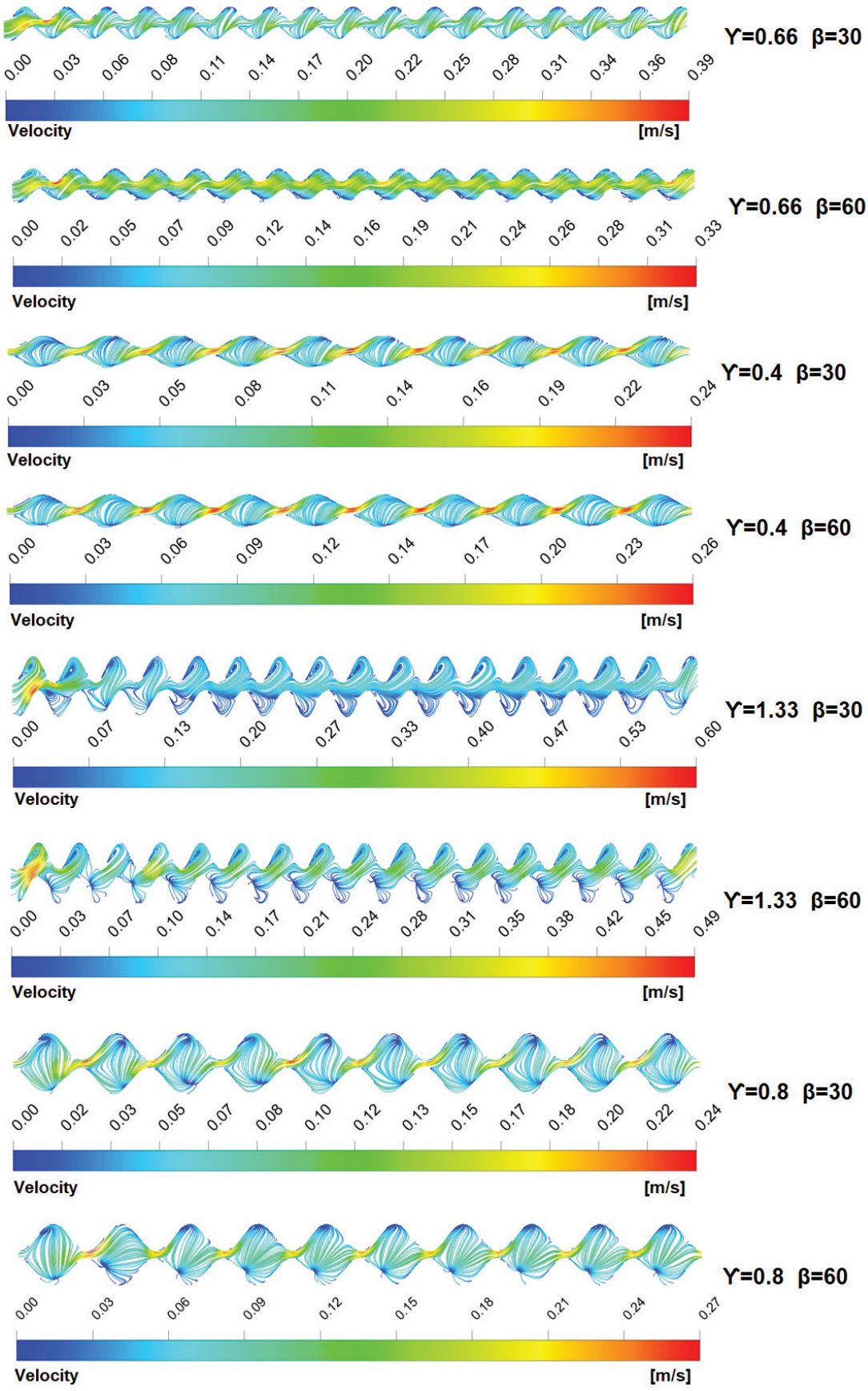

Figure 16. The effects of corrugation aspect ratio and chevron angle on the dynamic behavior of the flow field.

the opposite plate. Furthermore, this type of flow structure also has a spiral movement around itself.

The effect of geometric parameters on flow structure is shown in Figure 15. The increase of the chevron angle results in more spiral flows that promote the mixing and turbulence rate. Therefore, convection heat transfer rate and Nusselt number increased. Furthermore, comparison of 3D streamline structures reveals that increasing the aspect ratio favors crossflow structure in higher aspect ratio geometries, and cross flow behavior is more prominent than the helical one. Sarraf et al. [25] have reported similar streamline structure in their numerical work.

The effects of corrugation aspect ratio and chevron angle on the dynamic behavior of the flow field are presented with a streamline structure in Figure 16. The significant effect of the increased aspect ratio γ (higher amplitude and shorter wavelength) on the size and severity of lateral vortex (swirl flow) is clearly evident from the Figure 16. The intensity and size of these counter-rotating lateral vortices grows with increasing the aspect ratio which results in higher momentum transfer (convection heat transfer). The higher chevron angle makes the two-dimensional swirling flow to three-dimensional swirling flow [6].

CONCLUSION

This study focuses in detail on the effects of geometric parameters of a liquid-to-liquid plate heat exchanger on thermal boundary layer mitigation and frictional losses. A broad conjugate heat transfer numerical analyses were performed on corrugated plate heat exchangers with different aspect ratios and corrugation angles using Ansys Fluent commercial software. The numerical study was conducted at different Reynolds numbers from 500 to 3000. The main thermo-hydraulic parameters investigated are Nusselt number, isothermal friction factor, temperature distributions, thermal boundary layer, turbulence generation rate and mixing flow, 2D and 3D streamlines. The validation study of numerical simulation with previous experimental studies was carried out with data obtained from the literature which revealed a good agreement between numerical and experimental results. In the further part of the study, the variation of Nusselt number and friction factor has been analyzed with respect to Reynolds number. It has been found that the aspect ratio and chevron angle affect both the thermal and hydraulic performance of the heat exchanger. However, aspect ratio has a signification effect on turbulence and mixing flow generation. It has been observed that higher aspect ratio results in larger 3D vorticities and momentum transfer, leading to higher pumping power. The major results of this study are as follows:

- The maximum Nusselt number and friction factor were obtained for the geometry with aspect ratio of 1.33 and chevron angle of 60°. The chevron angle had a significant effect on the thermohydraulic performance of corrugated heat exchanger compared to the aspect ratio. The geometries with higher chevron angles have 1.3 - 2.06 times higher Nusselt numbers at the same aspect ratio and Reynolds numbers. In addition, the differentiation effect increases as the Reynolds number increases.
- When the axial temperature distributions were compared for various studied geometries, the lowest outlet temperatures were obtained to be 325.8 °C and 326.1 °C for geometries of 0.4-60° and 1.33-60° respectively. Also, the geometries with higher chevron angle had lower outlet temperatures.
- Geometries with higher chevron angle led to higher and even turbulence kinetic energy rate. The maximum kinetic energy rate of $3.53 \cdot 10^{-3}$ m^2/s^2 was obtained for the geometry of 1.33-60°. It was determined that for geometries with same aspect ratio and Reynolds number, the corrugate plate with chevron angle of 60° resulted in 35% more kinetic energy compared to the chevron angle of 30°.
- Fiction losses were significantly dependent on the chevron angle. However, increasing of chevron angle promoted the turbulence generation and mixing flow, but it intensified the frictional losses tremendously. Regarding the effect of aspect ratio on frictional losses, also a significant escalation in friction factor was seen with increasing of the aspect ratio. When aspect ratio increased from 0.4 to 1.33 for Reynolds Number of 1500 and chevron angle of 60, friction factor doubled.

In the literature, most of the research studies focus on the surface enlargement factor as an effective parameter, but the results of this study revealed that the main and crucial parameter that has a key effect on the convection heat transfer rate is the quality of turbulence generation and mixing flow. Another fact revealed by this study is the demand to trade of between the increasing of the turbulence flow and frictional losses in order to find the optimum thermo-hydraulic performance. A detailed insight into relationship between the flow structure and heat transfer rate will cause the development of more effective heat exchanger designs. Therefore, in-dept knowledge of turbulence generator geometries and their optimization is essential for thermal management applications. This question formed the main motivation of this research and future studies.

NOMENCLATURE

β	chevron or corrugation angle
b	corrugation depth or mean channel spacing (m)
λ	Corrugation Wavelength
L_W	Channel Width (mm)
L_{Ch}	Channel Length (mm)
$\Upsilon = 2b/\lambda$	Corrugation profile aspect ratio
ρ	Fluid density (kg/m^3)
P	Pressure (N/m^2)
τ	stress tensor
k_t	thermal conductivity (W/mK)

E	total energy per mass units (kJ/kg)
T	Temperature (k)
Re	Reynolds Number
D_e	Hydraulic Diameter
μ	dynamic viscosity, kg/ms
G	mass flux or mass velocity
$\dot{m}$	Mass flow rate (kg/s)
ΔP_f	Pressure drop in corrugated core section
A_c	Channel flow cross section area (m^2)
A	effective or actual heat transfer surface area, (m^2)
Q	Heat loads (W)
$LMTD$	logarithmic mean temperature difference, C
h	Convection heat transfer coefficient (W/m^2K)
U	Overall heat transfer coefficient (W/m^2K)
k	Thermal conductivity (W/mK)
t	plate thickness (mm)
f	friction coefficient
Nu	Nusselt Number

AUTHORSHIP CONTRIBUTIONS

Authors equally contributed to this work.

DATA AVAILABILITY STATEMENT

The authors confirm that the data that supports the findings of this study are available within the article. Raw data that support the finding of this study are available from the corresponding author, upon reasonable request.

CONFLICT OF INTEREST

The author declared no potential conflicts of interest with respect to the research, authorship, and/or publication of this article.

ETHICS

There are no ethical issues with the publication of this manuscript.

REFERENCES

[1] Kanaris AG, Mouza AA, Paras SV. Flow and heat transfer in narrow channels with corrugated walls a CFD code application. Chem Engineer Res Des 2005;83:460−468. [CrossRef]

[2] Bamorovat Abadi G, Moon C, Kim KC. Experimental study on single-phase heat transfer and pressure drop of refrigerants in a plate heat exchanger with metal-foam-filled channels. Appl Therm Eng 2016;102:423−431. [CrossRef]

[3] Kumar B, Soni A, Singh SN. Effect of geometrical parameters on the performance of Chevron type plate heat exchanger. Exp Therm Fluid Sci 2018;91:126−133. [CrossRef]

[4] Dovic D, Svaic S. Experimental and numerical study of the flow and heat transfer in plate heat exchanger channels. Int Refrig Air Cond Conf Purdue 2004;1−8.

[5] Turk C, Aradag S, Kakac S. Experimental analysis of a mixed-plate gasketed plate heat exchanger and artificial neural net estimations of the performance as an alternative to classical correlations. Int J Therm Sci 2016;109:263−269. [CrossRef]

[6] Gullapalli VS, Sundén B. CFD simulation of heat transfer and pressure drop in compact brazed plate heat exchangers. Heat Transf Engineer 2014;35:358−366. [CrossRef]

[7] Kanaris AG, Mouza AA, Paras SV. Flow and heat transfer prediction in a corrugated plate heat exchanger using a CFD code. Chem Engineer Technol 2006;29:923−930. [CrossRef]

[8] Septet C, El Achkar G, Le Metayer O, Hugo JM. Experimental investigation of two-phase liquid-vapor flows in additive manufactured heat exchanger. Appl Therm Engineer 2020;179:115638. [CrossRef]

[9] Gherasim I, Taws M, Galanis N, Nguyen CT. Heat transfer and fluid flow in a plate heat exchanger Part I. Experimental investigation. Int J Therm Sci 2011;50:1492−1498. [CrossRef]

[10] Yang J, Jacobi A, Liu W. Heat transfer correlations for single-phase flow in plate heat exchangers based on experimental data. Appl Therm Engineer 2017;113:1547−1557. [CrossRef]

[11] Khan TS, Khan MS, Chyu MC, Ayub ZH. Experimental investigation of single phase convective heat transfer coefficient in a corrugated plate heat exchanger for multiple plate configurations. Appl Therm Engineer 2010;30:1058−1065. [CrossRef]

[12] Gherasim I, Galanis N, Nguyen CT. Heat transfer and fluid flow in a plate heat exchanger. Part II: Assessment of laminar and two-equation turbulent models. Int J Therm Sci 2011;50:1499−1511. [CrossRef]

[13] Arsenyeva O, Kapustenko P, Tovazhnyanskyy L, Khavin G. The influence of plate corrugations geometry on plate heat exchanger performance in specified process conditions. Energy 2013;57:201−207. [CrossRef]

[14] Wang YN, Lee JP, Park MH, Jin BJ. A study on 3D numerical model for plate heat exchanger. Procedia Engineer 2017;174:188−194. [CrossRef]

[15] Longo GA, Mancin S, Righetti G, Zilio C, Ortombina L, Zigliotto M. Application of an artificial neural network (ANN) for predicting low-GWP refrigerant boiling heat transfer inside brazed plate heat exchangers (BPHE). Int J Heat Mass Transf 2020;160:120204. [CrossRef]

[16] Fernández-Seara J, Uhía FJ, Sieres J, Campo A. A general review of the Wilson plot method and its modifications to determine convection coefficients in heat exchange devices. Appl Therm Engineer 2007;27:2745−2757. [CrossRef]

[17] Lotfi B, Sundén B. Development of new finned tube heat exchanger: Innovative tube-bank design and thermohydraulic performance. Heat Transf Engineer 2020;41:1209−1231. [CrossRef]

[18] Han W, Saleh K, Aute V, Ding G. Numerical simulation and optimization of single-phase turbulent flow in chevron-type plate heat exchanger with sinusoidal corrugations. HVAC R Res 2011;17:186−197. [CrossRef]

[19] Tsai YC, Liu FB, Shen PT. Investigations of the pressure drop and flow distribution in a chevron-type plate heat exchanger. Int Comm Heat Mass Transf 2009;36:574−578. [CrossRef]

[20] Aradag S, Genc Y, Turk C. Comparative gasketed plate heat exchanger performance prediction with computations, experiments, correlations and artificial neural network estimations. Engineer Appl Comput Fluid Mech 2017;11:467−482. [CrossRef]

[21] Chien NB, Jong-Taek O, Asano H, Tomiyama Y. Investigation of experiment and simulation of a plate heat exchanger. Energy Procedia 2019;158:5635−5640. [CrossRef]

[22] Raja BD, Jhala RL, Patel V. Thermal-hydraulic optimization of plate heat exchanger: A multi-objective approach. Int J Therm Sci 2018;124:522−535. [CrossRef]

[23] Krishna Z, Sasanapuri A, Parkhi G, Varghese A. Ansys mosaic poly-hexcore mesh for high-lift aircraft configuration. 21st Annual CFD Symposium; 2019. pp. 1−11.

[24] Akkoca A, Sahin B, Tutar M. Effect of different wall functions on the prediction of flow and heat transfer characteristics in plate fin and tube heat exchangers. SUJEST 2005;20:77−86.

[25] Sarraf K, Launay S, Tadrist L. Complex 3D-flow analysis and corrugation angle effect in plate heat exchangers. Int J Therm Sci 2015;94:126−138. [CrossRef]

[26] Rios-Iribe EY, Cervantes-Gaxiola ME, Rubio-Castro E, Hernández-Calderón OM. Heat transfer analysis of a non-Newtonian fluid flowing through a plate heat exchanger using CFD. Appl Therm Engineer 2016;101:262−272. [CrossRef]

[27] Ansys. 5.2.1 Heat Transfer Theory. Available at: https://www.afs.enea.it/project/neptunius/docs/fluent/html/th/node107.htm. Accessed May 6, 2024.

[28] Muley A, Manglik RM, Metwally HM. Enhanced heat transfer characteristics of viscous liquid flows in a chevron plate heat exchanger. J Heat Transf 1999;121:1011−1017. [CrossRef]

[29] Moffat RJ. Describing the uncertainties in experimental results. Exp Therm Fluid Sci 1988;1:3−17. [CrossRef]